Supplement of Atmos. Chem. Phys., 17, 11041–11063, 2017
https://doi.org/10.5194/acp-17-11041-2017-supplement

Atmospheric Chemistry and Physics
Open Access
EGU

Supplement of

Pre-monsoon air quality over Lumbini, a world heritage site along the Himalayan foothills

Dipesh Rupakheti et al.

Correspondence to: Dipesh Rupakheti (dipesh.rupakheti@itpcas.ac.cn) and Shichang Kang (shichang.kang@lzb.ac.cn)

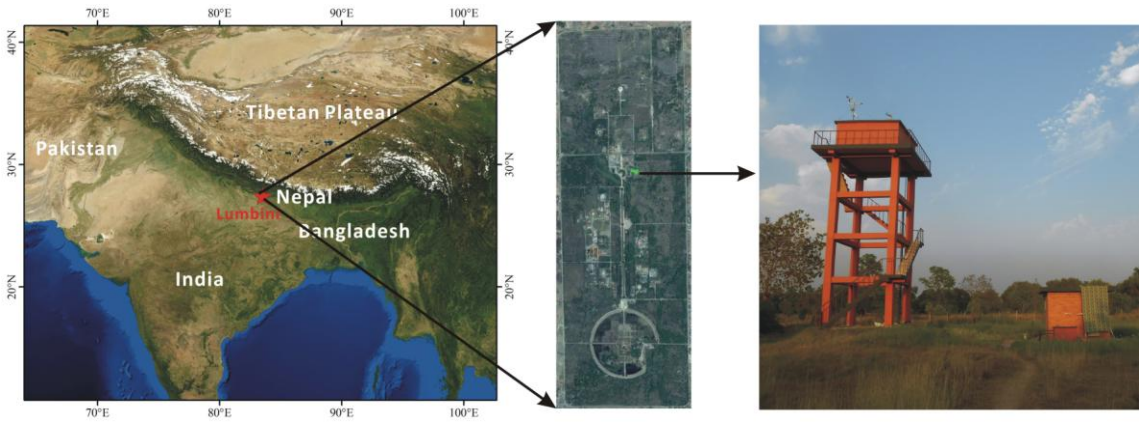

Figure S1. Location of sampling site in Lumbini in southern Nepal (left panel). The middle panel shows the Kenzo Tange Master Plan Area of Lumbini while the right panel shows the sampling tower in the Lumbini Master Plan Area. Lumbini lies in the Nepal's southern lowland plain or Terai region, termed as "bread basket of Nepal" due to the availability of very fertile land suitable for crop production, which forms the northern edge of the Indo-Gangetic Plain (IGP). The nearby premises of the monitoring site consist of the Lumbini International Research Institute (LIRI) main office and staff quarters. Further away is a museum, a local bus park for the visitors to Lumbini, the office of the Lumbini Development Trust, monasteries, and thinly forested area with grassland within the master plan area.

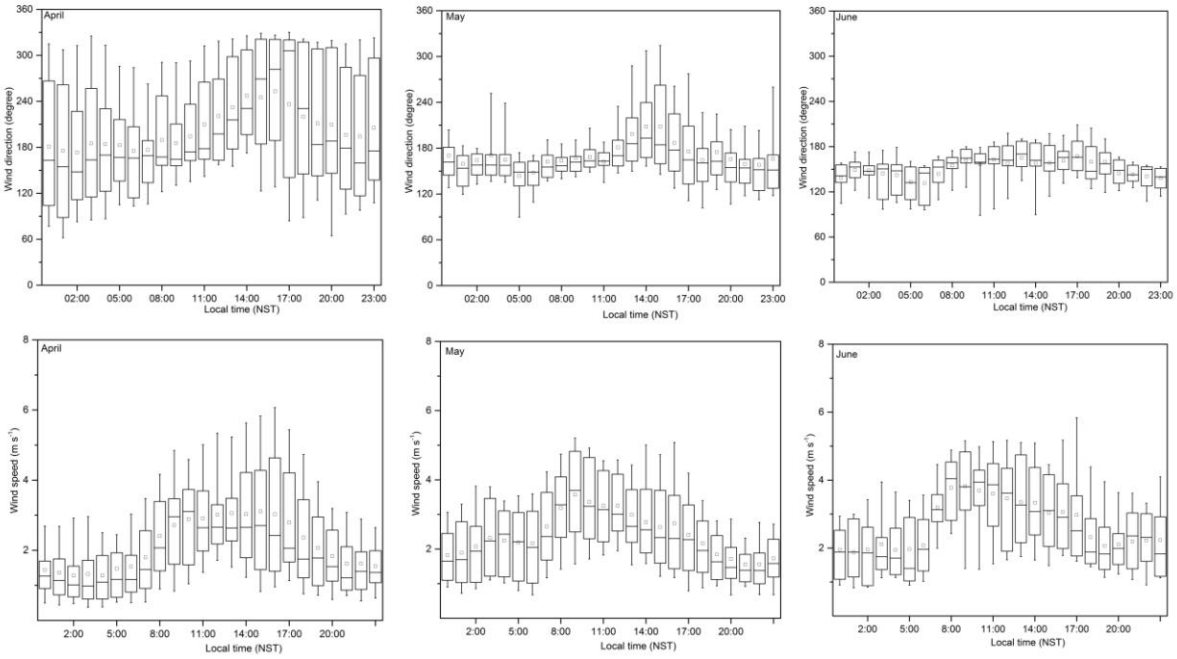

Figure S2. Monthly average diurnal variation of wind direction (degree) (upper panel) and wind speed (m s^{-1}) (lower panel), from observation, for the months of April, May and (1^{st}-15^{th}) June respectively. In each box, the lower and upper boundary represents 25^{th} and 75^{th} percentile respectively, top and bottom of the whisker represents 90^{th} and 10^{th} percentile respectively. The mid-line in each box represents median and the square mark represents the mean for each hour.

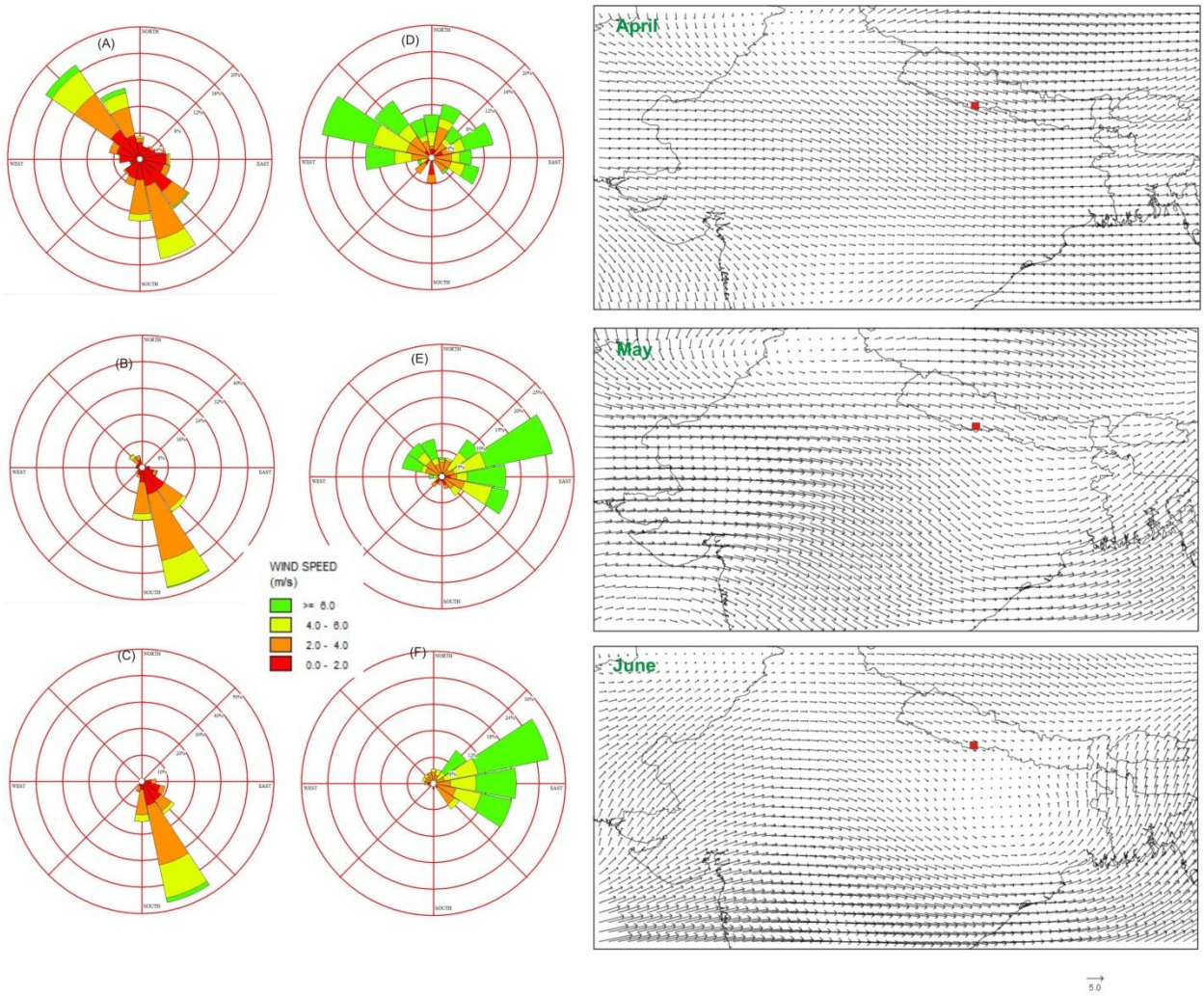

Figure S3: Wind rose of wind speed and wind direction obtained from the observation (A, B, C) and from the model (D, E, F) for the months of April, May and June 2013 respectively. The right panel shows the synoptic scale wind (850 hPa) during three months of the campaign.

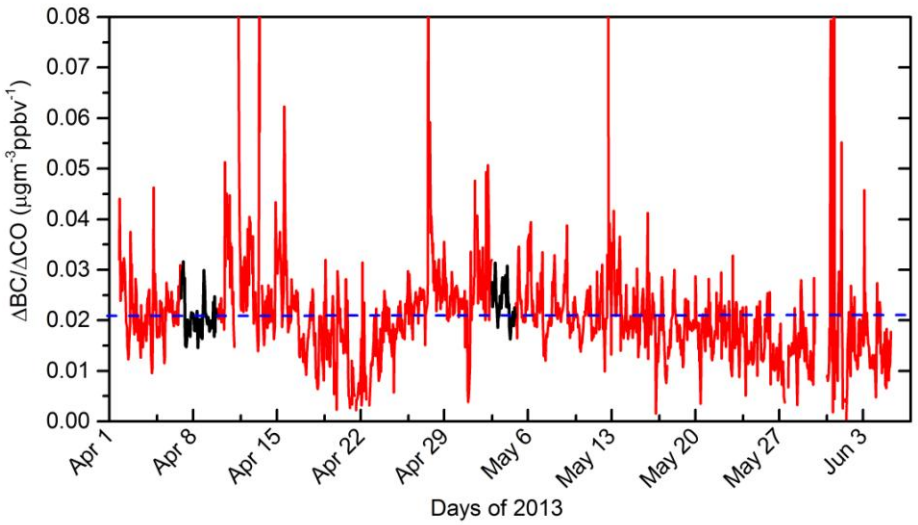

Figure S4: Time series of the ratio of hourly average BC concentrations to CO concentrations (ΔBC/ΔCO) observed in Lumbini (the black line refers to the two events discussed in the manuscript and blue line refers to the average ratio during sampling period).

Past studies used to compare the ratio with this study (Figure 4 in the revised manuscript) are (Subramanian et al., 2010;Verma et al., 2011;Verma et al., 2009;Dickerson et al., 2002;Val Martín et al., 2006;Hobbs et al., 2003;Girach et al., 2014;Badarinath et al., 2007;Cristofanelli et al., 2013;Pan et al., 2011;Kondo et al., 2011;Sahu et al., 2012;Antony Chen et al., 2001;Joshi et al., 2016;Park et al., 2005;Latha and Badarinath, 2004;Zhou et al., 2009;Retama et al., 2015) and are listed in the end of the supplementary materials file.

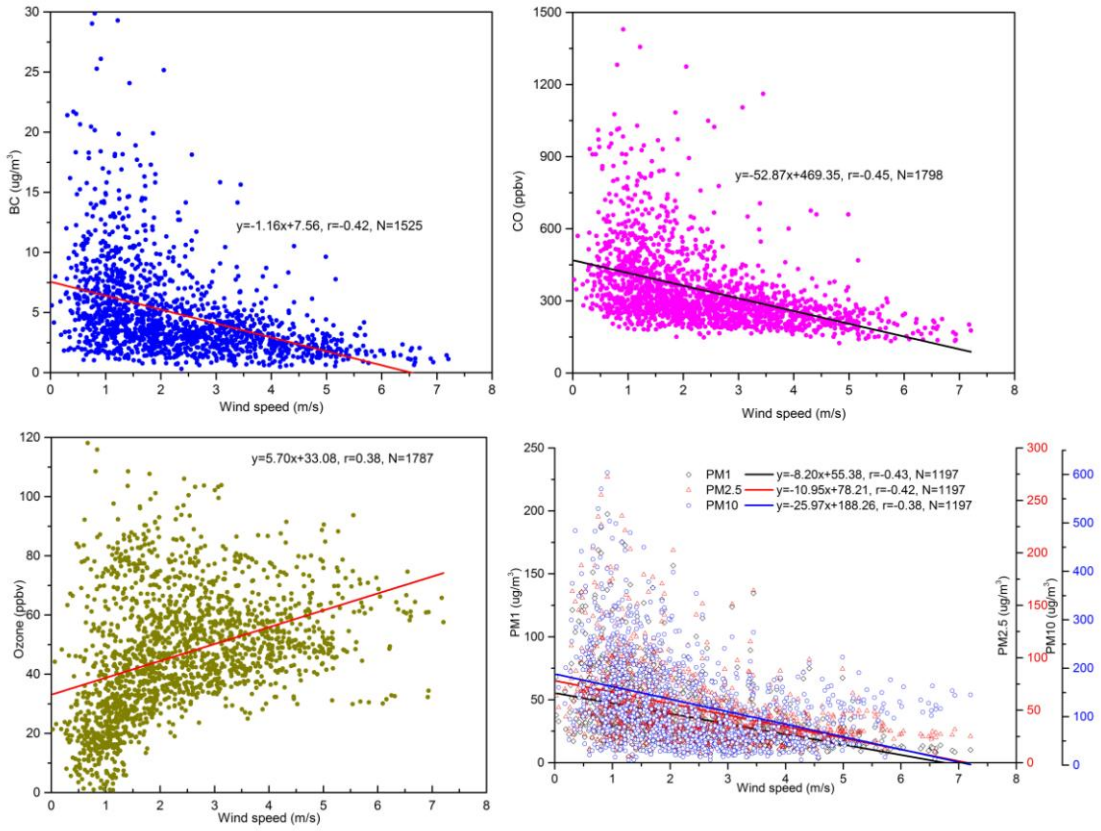

Figure S5: Relation plots of BC, CO, Ozone and PM with wind speed

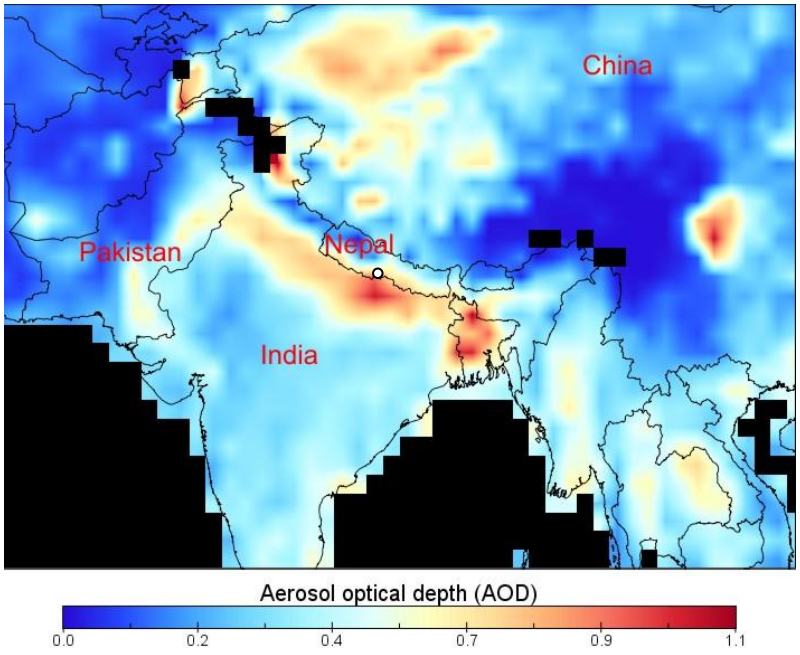

Figure S6. Aerosol optical depth in South Asia acquired with the MODIS instrument aboard TERRA satellite averaged during an intensive ground-based measurement period in Lumbini, Nepal (1 April- 15 June 2013). High aerosol loading can be seen over entire Ingo-Gangetic Plains (IGP). It is seen in the figure that Lumbini (a white circle with black border) is covered by the northern edge of an aerosol hotspot south of Lumbini.

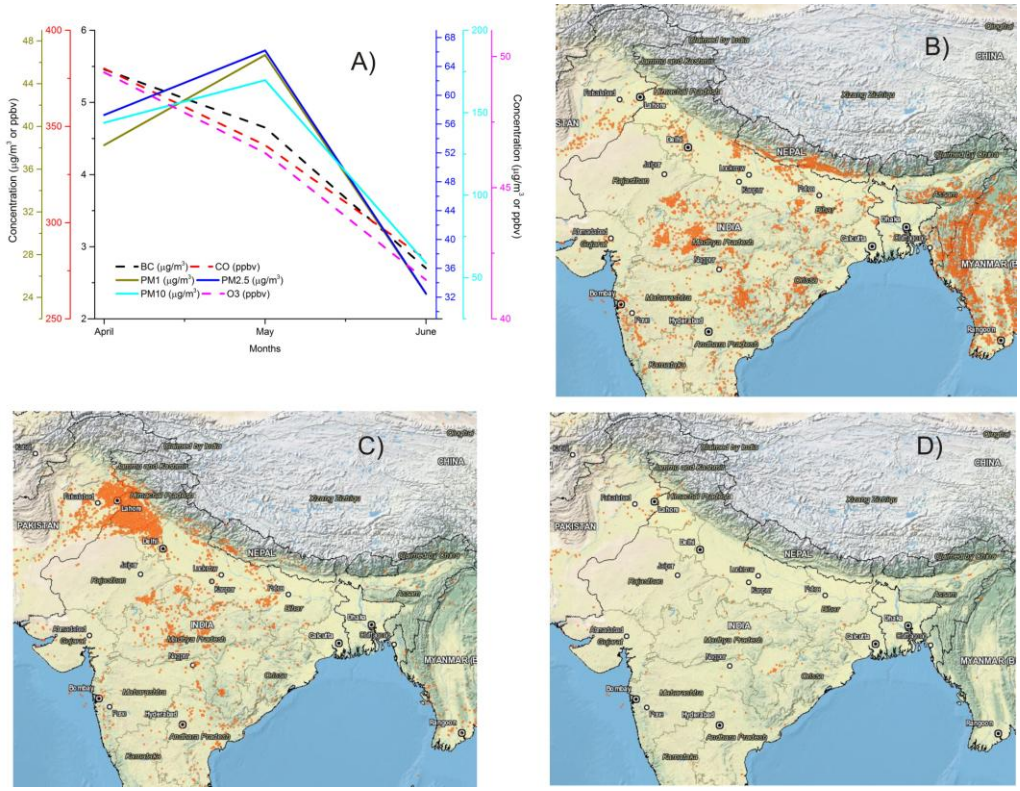

Figure S7. (A) Monthly average concentration of measured species (BC and PM fractions are in μg/m^3), (B), (C) and (D) refers to the monthly average fire points as retrieved by MODIS onboard TERRA satellite for April, May and June 2013, respectively.

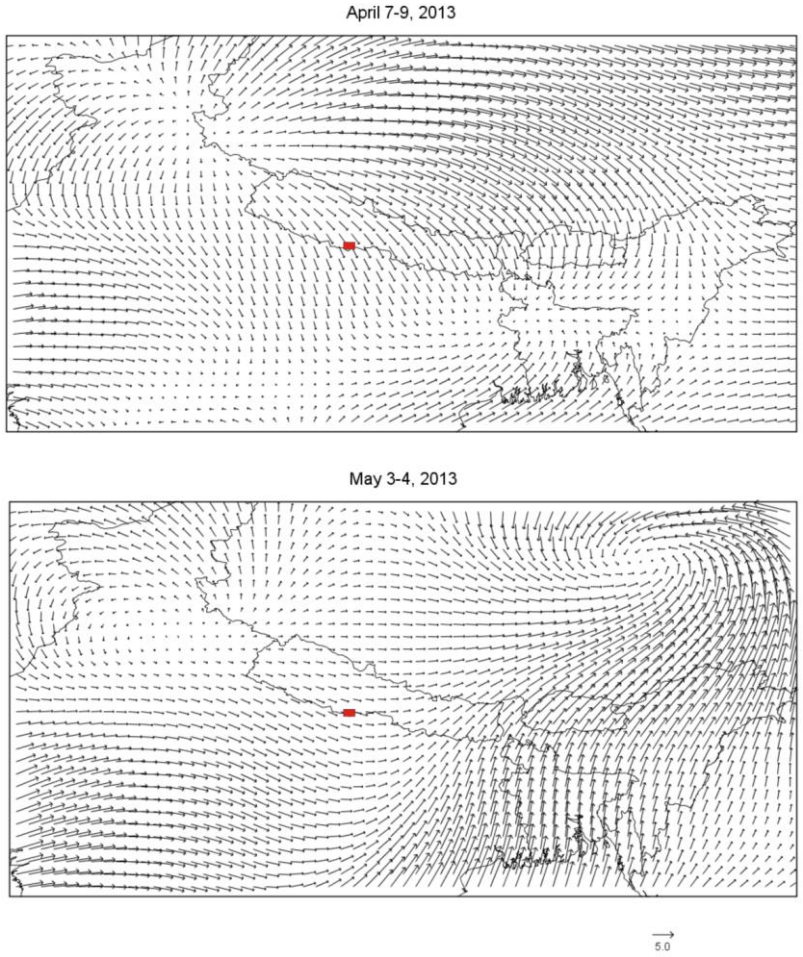

Figure S8. Synoptic scale winds during two events. The red box in the figure indicates the location of Lumbini.

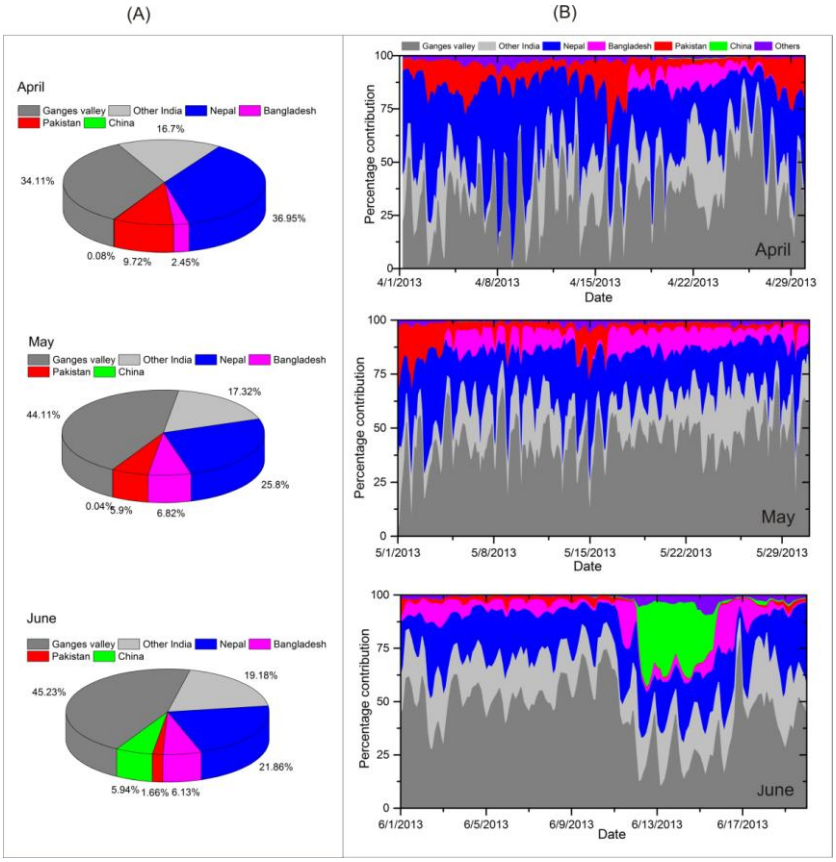

Figure S9. (A) Monthly average model estimated contributions of various source regions to average CO in Lumbini and (B) Time series of region tagged CO tracer during individual months.

References used for Figure 4

Antony Chen, L. W., Doddridge, B. G., Dickerson, R. R., Chow, J. C., Mueller, P. K., Quinn, J., and Butler, W. A.: Seasonal variations in elemental carbon aerosol, carbon monoxide and sulfur dioxide: Implications for sources, Geophys. Res. Lett., 28, 1711-1714, doi: 10.1029/2000gl012354, 2001.

Badarinath, K. V. S., Latha, K. M., Chand, T. R. K., Reddy, R. R., Gopal, K. R., Reddy, L. S. S., Narasimhulu, K., and Kumar, K. R.: Black carbon aerosols and gaseous pollutants in an urban area in North India during a fog period, Atmospheric Research, 85, 209-216, 10.1016/j.atmosres.2006.12.007, 2007.

Cristofanelli, P., Fierli, F., Marinoni, A., Calzolari, F., Duchi, R., Burkhart, J., Stohl, A., Maione, M., Arduini, J., and Bonasoni, P.: Influence of biomass burning and anthropogenic emissions on ozone, carbon monoxide and black carbon at the Mt. Cimone GAW-WMO global station (Italy, 2165 m a.s.l.), Atmos. Chem. Phys., 13, 15-30, doi: 10.5194/acp-13-15-2013, 2013.

Dickerson, R. R., Andreae, M. O., Campos, T., Mayol-Bracero, O. L., Neususess, C., and Streets, D. G.: Analysis of black carbon and carbon monoxide observed over the Indian Ocean: Implications for emissions and photochemistry, Journal of Geophysical Research: Atmospheres, 107, INX2 16-11-INX12 16-11, 10.1029/2001JD000501, 2002.

Girach, I. A., Nair, V. S., Babu, S. S., and Nair, P. R.: Black carbon and carbon monoxide over Bay of Bengal during W_ICARB: Source characteristics, Atmospheric Environment, 94, 508-517, http://dx.doi.org/10.1016/j.atmosenv.2014.05.054, 2014.

Hobbs, P. V., Sinha, P., Yokelson, R. J., Christian, T. J., Blake, D. R., Gao, S., Kirchstetter, T. W., Novakov, T., and Pilewskie, P.: Evolution of gases and particles from a savanna fire in South Africa, J. Geophys. Res., 108, D13, doi:10.1029/2002JD002352, 2003.

Joshi, H., Naja, M., Singh, K., Kumar, R., Bhardwaj, P., Babu, S. S., Satheesh, S., Moorthy, K. K., and Chandola, H.: Investigations of aerosol black carbon from a semi-urban site in the Indo-Gangetic Plain region, Atmos. Environ., 125, 346-359, doi: 10.1016/j.atmosenv.2015.04.007, 2016.

Kondo, Y., Matsui, H., Moteki, N., Sahu, L., Takegawa, N., Kajino, M., Zhao, Y., Cubison, M. J., Jimenez, J. L., Vay, S., Diskin, G. S., Anderson, B., Wisthaler, A., Mikoviny, T., Fuelberg, H. E., Blake, D. R., Huey, G., Weinheimer, A. J., Knapp, D. J., and Brune, W. H.: Emissions of black carbon, organic, and inorganic aerosols from biomass burning in North America and Asia in 2008, Journal of Geophysical Research: Atmospheres, 116, n/a-n/a, 10.1029/2010JD015152, 2011.

Latha, K. M., and Badarinath, K. V. S.: Correlation between black carbon aerosols, carbon monoxide and tropospheric ozone over a tropical urban site, Atmospheric Research, 71, 265-274, http://dx.doi.org/10.1016/j.atmosres.2004.06.004, 2004.

Pan, X. L., Kanaya, Y., Wang, Z. F., Liu, Y., Pochanart, P., Akimoto, H., Sun, Y. L., Dong, H. B., Li, J., Irie, H., and Takigawa, M.: Correlation of black carbon aerosol and carbon monoxide in the high-altitude environment of Mt. Huang in Eastern China, Atmos. Chem. Phys., 11, 9735-9747, doi: 10.5194/acp-11-9735-2011, 2011.

Park, S. S., Harrison, D., Pancras, J. P., and Ondov, J. M.: Highly time-resolved organic and elemental carbon measurements at the Baltimore Supersite in 2002, J. Geophys. Res., 110, D07S06, doi: 10.1029/2004jd004610, 2005.

Retama, A., Baumgardner, D., Raga, G. B., McMeeking, G. R., and Walker, J. W.: Seasonal and diurnal trends in black carbon properties and co-pollutants in Mexico City, Atmos. Chem. Phys., 15, 9693-9709, doi: 10.5194/acp-15-9693-2015, 2015.

Sahu, L. K., Kondo, Y., Moteki, N., Takegawa, N., Zhao, Y., Cubison, M. J., Jimenez, J. L., Vay, S., Diskin, G. S., Wisthaler, A., Mikoviny, T., Huey, L. G., Weinheimer, A. J., and Knapp, D. J.: Emission characteristics of black carbon in anthropogenic and biomass burning plumes over California during ARCTAS-CARB 2008, J. Geophys. Res., 117, D16302, n/a-n/a, doi: 10.1029/2011jd017401, 2012.

Subramanian, R., Kok, G., Baumgardner, D., Clarke, A., Shinozuka, Y., Campos, T., Heizer, C., Stephens, B., Foy, B. d., and Voss, P. B.: Black carbon over Mexico: the effect of atmospheric transport on mixing state, mass absorption cross-section, and BC/CO ratios, Atmospheric Chemistry and Physics, 10, 219-237, 2010.

Val Martín, M., Honrath, R. E., Owen, R. C., Pfister, G., Fialho, P., and Barata, F.: Significant enhancements of nitrogen oxides, black carbon, and ozone in the North Atlantic lower free troposphere resulting from North American boreal wildfires, J. Geophys. Res., 111, D23S60, n/a-n/a, doi: 10.1029/2006jd007530, 2006.

Verma, R. L., Kondo, Y., Oshima, N., Matsui, H., Kita, K., Sahu, L. K., Kato, S., Kajii, Y., Takami, A., and Miyakawa, T.: Seasonal variations of the transport of black carbon and carbon monoxide from the Asian continent to the western Pacific in the boundary layer, J. Geophys. Res., 116, D21307, doi: 10.1029/2011jd015830, 2011.

Verma, S., Worden, J., Payra, S., Jourdain, L., and Shim, C.: Characterizing the long-range transport of black carbon aerosols during Transport and Chemical Evolution over the Pacific (TRACE-P) experiment, Environmental monitoring and assessment, 154, 85-92, 10.1007/s10661-008-0379-2, 2009.

Zhou, X., Gao, J., Wang, T., Wu, W., and Wang, W.: Measurement of black carbon aerosols near two Chinese megacities and the implications for improving emission inventories, Atmospheric Environment, 43, 3918-3924, 10.1016/j.atmosenv.2009.04.062, 2009.